

Research Article Implant Science



Received: Jul 15, 2022
Revised: Sep 25, 2022
Accepted: Oct 12, 2022
Published online: Nov 21, 2022

*Correspondence:

Jae-Kook Cha

Department of Periodontology, College of Dentistry, Yonsei University, 50-1 Yonsei-ro, Seodaemun-gu, Seoul 03722, Korea.

Email: chajaeekook@yuhs.ac

Tel: +82-2-2228-3191

Fax: +82-2-392-0398

*Xiang Jin and Jin-Young Park contributed equally to this manuscript.

Copyright © 2023. Korean Academy of Periodontology

This is an Open Access article distributed under the terms of the Creative Commons Attribution Non-Commercial License (<https://creativecommons.org/licenses/by-nc/4.0/>).

ORCID iDs

Jin-Young Park <https://orcid.org/0000-0002-6408-1618>

Jung-Seok Lee <https://orcid.org/0000-0003-1276-5978>

Ui-Won Jung <https://orcid.org/0000-0001-6371-4172>

Seong-Ho Choi <https://orcid.org/0000-0001-6704-6124>

Jae-Kook Cha <https://orcid.org/0000-0002-6906-7209>

Funding

This work was supported by the Korea Medical Device Development Fund grant funded by the

Tissue integration patterns of non-crosslinked and crosslinked collagen membranes: an experimental *in vivo* study

Xiang Jin^{1,†}, Jin-Young Park ^{1,2,†}, Jung-Seok Lee ^{1,2}, Ui-Won Jung ¹,
Seong-Ho Choi ^{1,2}, Jae-Kook Cha ^{1,2,*}

¹Department of Periodontology, Research Institute of Periodontal Regeneration, Yonsei University College of Dentistry, Seoul, Korea

²Innovation Research and Support Center for Dental Science, Yonsei University Dental Hospital, Seoul, Korea

ABSTRACT

Purpose: Non-crosslinked and crosslinked collagen membranes are known to exhibit distinct degradation characteristics, resulting in contrasting orientations of the adjacent tissues and different biological processes. The aim of this study was to conduct a histomorphometric assessment of non-crosslinked and crosslinked collagen membranes regarding neovascularization, tissue integration, tissue encapsulation, and biodegradation.

Methods: Guided bone regeneration was performed using either a non-crosslinked (BG) or a crosslinked collagen membrane (CM) in 15 beagle dogs, which were euthanized at 4, 8, and 16 weeks (n=5 each) for histomorphometric analysis. The samples were assessed regarding neovascularization, tissue integration, encapsulation, the remaining membrane area, and pseudoperiosteum formation. The BG and CM groups were compared at different time periods using nonparametric statistical methods.

Results: The remaining membrane area of CM was significantly greater than that of BG at 16 weeks; however, there were no significant differences at 4 and 8 weeks. Conversely, the neovascularization score for CM was significantly less than that for BG at 16 weeks. BG exhibited significantly greater tissue integration and encapsulation scores than CM at all time periods, apart from encapsulation at 16 weeks. Pseudoperiosteum formation was observed in the BG group at 16 weeks.

Conclusions: Although BG membranes were more rapidly biodegraded than CM membranes, they were gradually replaced by connective tissue with complete integration and maturation of the surrounding tissues to form dense periosteum-like connective tissue. Further studies need to be performed to validate the barrier effect of the pseudoperiosteum.

Keywords: Bone regeneration; Bone substitutes; Collagen; Cross-linking reagents; Ethyldimethylaminopropyl carbodiimide

INTRODUCTION

The principle of guided bone regeneration (GBR) can be primarily explained by the role of the barrier membrane. The barrier membrane covers a bone defect, thereby creating a

Korean government (the Ministry of Science and ICT, the Ministry of Trade, Industry and Energy, the Ministry of Health & Welfare, the Ministry of Food and Drug Safety) (Project Number: KMDF_PR_20200901_0240), and also by a grant of the Korea Health Technology R&D Project through the Korea Health Industry Development Institute (KHIDI), funded by the Ministry of Health & Welfare, Republic of Korea (grant number: HI20C2114).

Data Availability

The data of this study are available upon request from the corresponding author.

Conflict of Interest

No potential conflict of interest relevant to this article was reported.

Author Contributions

Conceptualization: Jae Kook Cha; Formal analysis: Xiang Jin, Jin Young Park; Funding acquisition: Ui Won Jung; Investigation: Jae Kook Cha; Methodology: Jae Kook Cha; Project administration: Jae Kook Cha; Resources: Jae Kook Cha; Supervision: Jung Seok Lee, Seong Ho Choi, Ui Won Jung, Jae Kook Cha; Writing - original draft: Xiang Jin, Jin Young Park; Writing - review & editing: Jung Seok Lee, Jae Kook Cha.

secluded space for bone-forming cells to proliferate and regenerate the alveolar bone, and at the same time, it occludes the overlying soft tissues and prevents them from infiltrating the defect space. Resorbable collagen membranes are now the most frequently used barrier membranes for GBR [1] due to the absence of a need for membrane removal, the ease of surgical manipulation and spontaneous healing after the incidence of membrane exposure. Nonetheless, the use of resorbable membranes is limited by their low capacity for space maintenance and rapid resorption rate [2]. Therefore, attempts have been made to slow the resorption rate and prolong the duration of action.

Crosslinking of collagen fibers has been advocated to improve resistance to enzymatic degradation. Various physical and chemical crosslinking agents have been tested, such as ribose, glutaraldehyde, and ultraviolet rays; however, many of them have exhibited cytotoxicity and compromised biocompatibility [3]. Recent advances have produced membranes with improved biocompatibility and endurance to degradation by utilizing bioinert crosslinking agents such as 1-ethyl-3-(3-dimethylaminopropyl) carbodiimide (EDC) [4,5]. Meanwhile, there is ample scientific evidence for the use of non-crosslinked collagen membranes, which are well known to show good biocompatibility and the ability to closely integrate with the surrounding tissues [6,7].

From an evaluation of the clinical data, it is difficult to determine whether crosslinking of the collagen membrane enhances the outcomes of GBR. A recent meta-analysis showed that crosslinked collagen membranes were more effective than non-crosslinked membranes when used for vertical ridge augmentation [8], whereas another meta-analysis reported no significant difference between the 2 types of collagen membranes concerning the gain in bone volume [9]. Nevertheless, heterogeneity among studies means that this comparison is susceptible to bias. In addition, it is difficult to study membrane degradation clinically due to ethical issues. Therefore, a well-designed animal study is indicated to observe the healing pattern and tissue response surrounding the barrier membranes.

Most preclinical studies on resorbable membrane degradation and the tissue response have been performed using rat subcutaneous models [10-12]. Those studies showed that the rate of biodegradation was the fastest for non-crosslinked collagen membranes, although the amount of tissue integration and vascularization was the highest compared to other crosslinked collagen and synthetic membranes. Nevertheless, subcutaneous models lack clinical representativeness, since in GBR application, the membrane is in contact with the alveolar bone, oral mucosa, and the bone substitute. In the literature, there is a surprising lack of well-designed animal studies comparing the degradation and healing pattern around non-crosslinked and crosslinked collagen membranes.

Therefore, the aim of this study was to conduct histomorphometric assessments of the natural and crosslinked collagen membranes regarding neovascularization, tissue integration, tissue encapsulation, and biodegradation.

MATERIALS AND METHODS

Ethical statement and experimental animals

Fifteen beagle dogs were used for this study, aged 15–24 months and weighing 15 kg. The animals were raised under standard laboratory conditions (room temperature of

15°C–20°C and humidity of >30%) and fed a standardized soft diet throughout the study. The experimental approaches and protocols were authorized by the Institutional Animal Care and Use Committee, Yonsei Medical Center in Seoul, South Korea (approval no. 2016–0053), and was carried out according to the modified Animal Research: Reporting of In Vivo Experiments (ARRIVE) guidelines for research in preclinical settings.

Study materials

Collagen membranes

Two types of collagen membranes were compared in this study. Firstly, a non-crosslinked collagen membrane (Bio-Gide; Geistlich Pharma AG, Wolhusen, Switzerland) (BG) was composed of type I and III collagen derived from porcine peritoneum. This membrane has a bilayer structure consisting of a dense outer layer and a spongy inner layer. The second collagen membrane was a crosslinked collagen membrane composed of type 1 collagen, crosslinked using EDC (Collagen Membrane-P; Genoss, Suwon, Korea) (CM). This membrane had a uniform structure. Crosslinking was performed by immersing the membrane in 5 mM EDC solution at 4°C for 24 hours, followed by thorough washing and lyophilization (**Figure 1**).

Bone graft material

A collagenated-block bone graft material was used in this study (Mastergraft Putty, Medtronic, Minneapolis, MN, USA). This material is a synthetic biphasic calcium phosphate consisting of 15% hydroxyapatite and 85% β -tricalcium phosphate, which is equally distributed throughout ultra-purified resorbable type I bovine collagen.

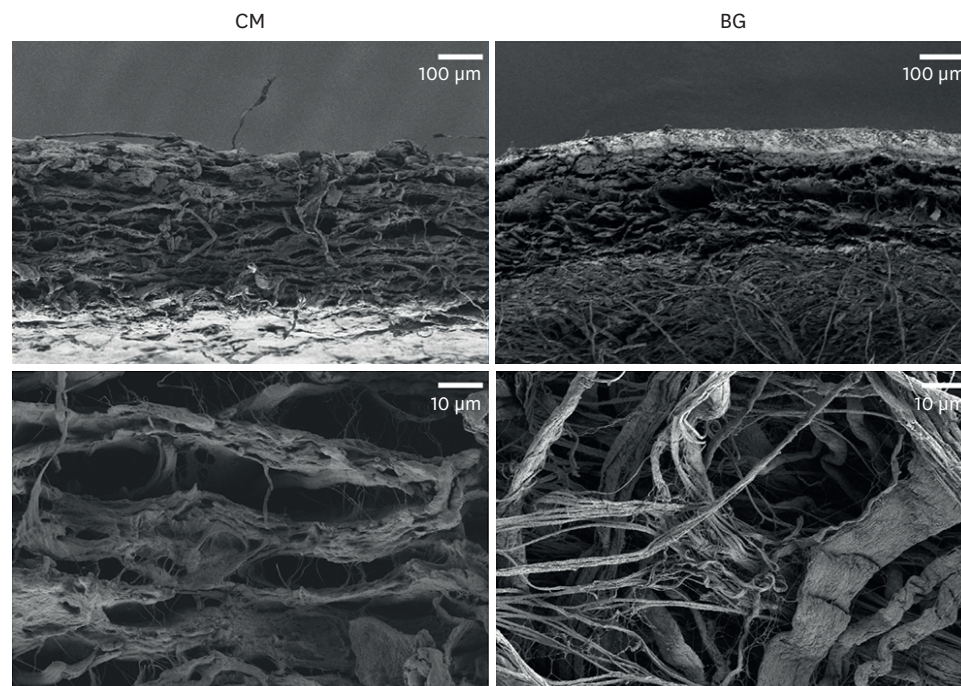


Figure 1. Scanning electron micrograph images of the non-crosslinked collagen membrane (Bio-Gide; Geistlich Pharma AG, Wolhusen, Switzerland) (BG) and the crosslinked collagen membrane (Collagen membrane-P; Genoss, Suwon, Korea) (CM) at $\times 100$ and $\times 1,000$ magnifications. CM: crosslinked collagen membrane, BG: Bio-Gide.

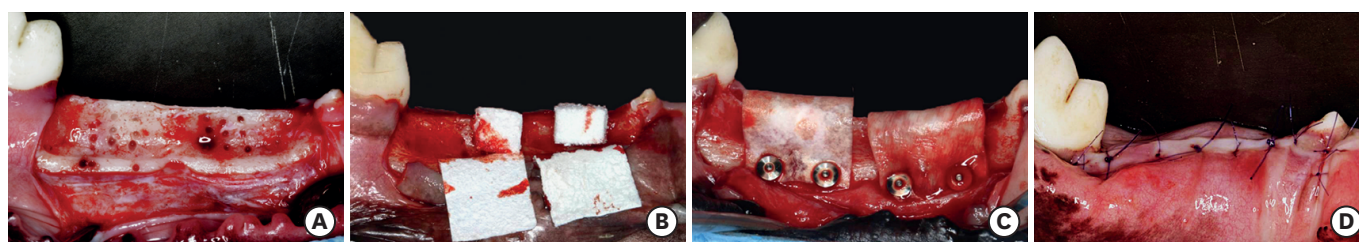


Figure 2. The surgical procedure. (A) A full-thickness flap was elevated, and the alveolar bone bed was decorticated. (B) A collagenated synthetic bone block was placed in each experimental site (Mastergraft Putty; Medtronic, Minneapolis, MN, USA). (C) The bone substitutes were covered by 2 different membranes according to group allocation; left: crosslinked collagen membrane, right: a non-crosslinked collagen membrane, and fixed with 2 titanium pins. (D) Primary closure was achieved.

Study design

In 15 beagle dogs, a chronic narrow ridge was induced on 1 side by extraction of the second, third, and fourth premolars. After 8 weeks of healing, GBR was performed on 2 sites unilaterally (**Figure 2**). The 2 experimental groups—i) the BG group and ii) the CM group—were randomly allocated to either the mesial or the distal site of the ridge. Animals were euthanized at 4, 8, and 16 weeks (n=5 for each period).

Surgical protocol

General anesthesia was induced using an intravenous injection of medetomidine (0.75 mg/kg; Tomidin, Provet Veterinary Products) and alfaxalone (2 mg/kg; Jurox). Inhalation anesthesia was performed using isoflurane (Forane, Choongwae Pharmaceutical, Seoul, Korea). Local anesthesia was performed by infiltration of lidocaine hydrochloride (1:100,000) (Kwang Myung Pharm Co., Ltd., Seoul, Korea). Supragingival scaling was performed prior to the extraction of the second, third, and fourth premolars. The buccal plates of the extraction sockets were removed using a tungsten carbide bur to create a narrow ridge.

After 8 weeks of healing, GBR was performed in a unilateral edentulous ridge. A crestal incision and 2 vertical incisions were made to raise a full-thickness mucoperiosteal flap. The synthetic block graft materials were trimmed to the size of 6×5×5 mm and then applied to each bone defect (**Figure 2**). The graft materials were covered with either BG or CM trimmed to the size of 12×18 mm, followed by fixation of the membranes using 2 titanium pins (Membrane Pin; Dentium, Suwon, Korea) (**Figure 1**). The flap was advanced with periosteal releasing incisions, and tension-free primary closure was achieved with sutures (4-0 Monosyn, B. Braun, Melsungen, Germany). The specimens were euthanized at 4, 8, and 16 weeks postoperatively for histologic processing.

Histologic processing

Block samples were obtained from the unilateral mandible and fixed in 10% neutral buffered formalin for 2 weeks. The samples were embedded in acrylic resin (Technovit 7200 VLC; Heraeus Kulzer, South Bend, IN, USA) and ground sections were produced from the most central portion of the defect and prepared at the thickness of 45 μm. The samples were stained with Goldner's trichrome and digitally scanned at ×200 magnification (Pannoramic 250 Flash III; 3D HISTECH, Budapest, Hungary). The scanned images were examined using dedicated software (Case Viewer; 3D HISTECH).

Table 1. Parameters evaluated during histopathological scoring of the samples

General tissue reaction	Scoring system
Pseudoperiosteum	–, absent; +, present in ≥10% of the target section; ++, present in ≥20% of the target section; and +++, present in ≥50% of the target section.
Neovascularization	The number of capillaries within the area of the membrane: 0, none; 1, minimal proliferation of capillaries; 2, formation of 4–7 capillary structures; 3, a wide band of capillaries; and 4, a substantial band of capillaries.
Encapsulation	Encapsulation was descriptively assessed based on the thickness of mature collagen surrounding the membrane and scored as follows: 0, none; 1, a narrow band; 2, a moderate band; 3, a thick band; and 4, a substantial band.
Tissue integration	The degree of tissue growth into the membrane: 0, none; 1, slight; 2, moderate; 3, marked; and 4, complete/severe.

Histomorphometric measurements

Histomorphometric measurements were performed by a trained investigator (X.J.) who was blinded to the experimental groups, and outcomes were reviewed by 2 other investigators (J.K.C. and J.Y.P.). A semi-quantitative and descriptive score was given for the local tissue response at the implantation sites according to the ISO 10993-6 guidelines [10] (**Table 1**). Quantitative measurements of the remaining membrane thickness and area were made using Adobe Photoshop CS5 (Adobe Systems, San Jose, CA, USA) was used. The following variables were assessed for each sample:

- Remaining membrane thickness (mm): measured at 5 points equally dividing the defect site to obtain a mean value
- Remaining membrane area (mm²): the area of the membrane remnants at the entire grafted site
- Neovascularization: the number of capillaries within the area of the membrane at the augmented site
- Encapsulation: the thickness of mature collagen surrounding the membrane
- Tissue integration: the degree of tissue growth into the membrane
- Pseudoperiosteum: the formation of periosteum-like tissues replacing the membrane, characterized by dense fibrous layer of connective tissues overlying a cellular layer

Statistical analysis

All measurement data are presented as mean ± standard deviation. Statistical analyses were performed using SPSS version 21.0 (IBM Corp, Armonk, NY, USA). Nonparametric tests were applied given the descriptive nature of the study. The Mann-Whitney *U* test and Wilcoxon signed rank test were used for inter-group and intra-group comparisons, respectively. The differences were deemed statistically significant when the *P* values were less than 0.05.

RESULTS

Clinical observation

Surgical wound healing was uneventful, without complications such as wound dehiscence, severe swelling, or bleeding.

Histological observation

Week 4

At week 4, membrane remnants of both BG and CM could be observed, although BG underwent substantially greater resorption than CM (**Figure 3**). Regarding angiogenesis, blood vessel formation was scanty evident within the membrane space of BG, whereas CM showed no signs of vascularization (**Figure 4**). BG was closely integrated with the surrounding

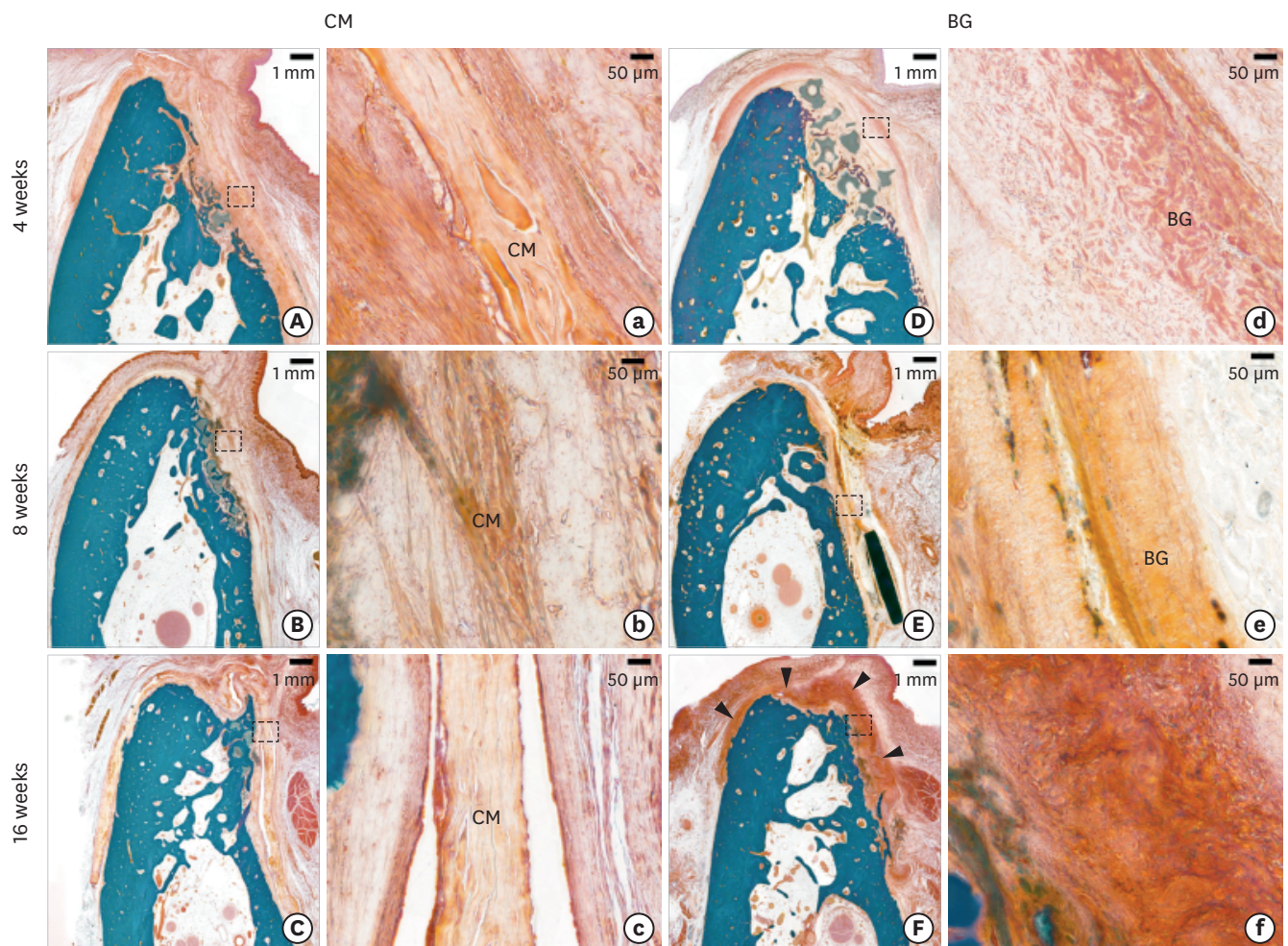


Figure 3. Histological images obtained at 4, 8, and 16 weeks. (A-F) Low-magnification images from the CM and BG groups. The black triangles indicate the pseudoperiosteum. Histological images obtained at 4, 8, and 16 weeks. (a-f) High-magnification images of the areas highlighted in panels (A-F). CM: crosslinked collagen membrane, BG: Bio-Gide.

connective tissues and interstitial matrix. In addition, the fibrous tissues surrounding BG appeared significantly thicker compared to those surrounding CM (**Figure 3**).

Week 8

At week 8, both CM and BG appeared to have been resorbed significantly (**Figure 3**). Regarding angiogenesis, the space once occupied by BG contained numerous blood vessels, whereas few blood vessels could be seen within the space of CM (**Figure 4**). It was evident that BG had been almost completely integrated with the surrounding tissues, which appeared to have greater maturity and thickness than at 4 weeks (**Figure 3**). For CM, the degree of tissue integration appeared similar to that at 4 weeks, and the surrounding fibrous tissues also showed similar maturity to that at 4 weeks.

Week 16

Even at 16 weeks, some of the samples showed unresorbed remnants of CM, which was still unintegrated with the surrounding tissues (**Figure 3**). Conversely, it appeared that BG was almost fully resorbed, with no signs of membrane remnants. Nevertheless, the membrane space of BG was occupied by a mature dense fibrous layer of connective tissue, which

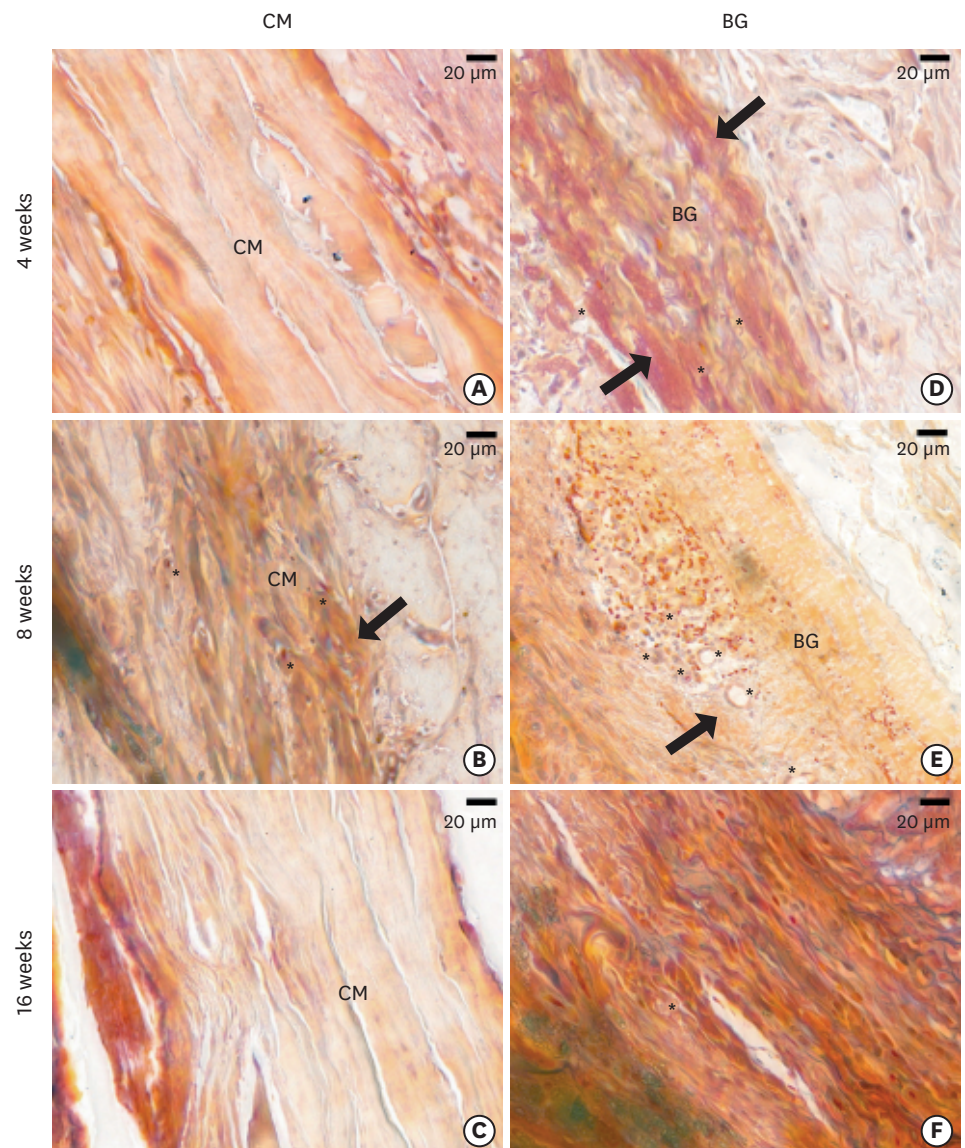


Figure 4. High-magnification images of a representative sample from each group. Neovascularization is indicated by an asterisk. The black arrows indicate tissue integration of the surrounding connective tissues with the membrane. CM: crosslinked collagen membrane, BG: Bio-Gide.

resembled the periosteum. It could be seen that the remaining superficial bone graft particles were entangled within this layer. Regarding angiogenesis, the pseudoperiosteum of BG was richly vascularized, whereas that of CM showed a scarce distribution of vessels (**Figure 4**).

Histomorphometric analysis

Neovascularization

At 4 and 8 weeks postoperatively, no statistically significant differences were found in the neovascularization score between CM and BG ($P=0.053$ and $P=0.08$, respectively) (**Table 2**). At week 16, the neovascularization score was significantly higher for BG than for CM ($P=0.007$). There was no significant difference in neovascularization scores between the different time points for both membranes ($P>0.05$).

Table 2. Results of the histological analysis

Time point (wk)	CM			BG		
	4 wk	8 wk	16 wk	4 wk	8 wk	16 wk
Pseudoperiosteum	–	–	–	–	–	++
Neovascularization	0±0	0.4±0.55	0.6±0.55	1.40±1.52	1.60±1.14	2.60±0.55 ^{c)}
Encapsulation	1±0	1.4±0.55	2.4±1.14	2±0.71 ^{c)}	2.2±0.45 ^{c)}	3.2±0.84
Tissue integration	0±0	0.4±0.55	0.8±0.45 ^{a)}	2.8±0.45 ^{c)}	2±1 ^{c)}	4±0 ^{a,b,c)}

CM: crosslinked collagen membrane, BG: Bio-Gide.

Numbers represent the mean ± standard deviation of the parameters using the following scoring system: 0: none, 1: slight, 2: moderate, 3: marked, and 4: complete/severe. The general tissue reaction was evaluated using the following scoring system: –, not present; +, present in ≥10% of the viewed area; ++, present in ≥20% of the viewed area; and +++, present in ≥50% of the viewed area.

^{a)}Significant intragroup difference between week 4 and week 16; ^{b)}Significant intragroup difference between week 8 and week 16; ^{c)}Significant intergroup difference at the same observation period.

Encapsulation

At weeks 4 and 8, the encapsulation scores of BG were significantly higher than those of CM ($P=0.017$ and $P=0.042$, respectively) (**Table 2**). However, at week 16, there was no significant difference between BG and CM ($P>0.05$). From weeks 4 to 16, the encapsulation score of both membranes tended to increase; however, the difference was not significant ($P>0.05$).

Tissue integration

The tissue integration score of the BG group was significantly higher than that of the CM group at weeks 4, 8, and 16 ($P=0.004$, $P=0.021$, and $P=0.004$, respectively) (**Table 2**). In the CM group, the tissue integration score significantly increased by week 16 compared to week 4 ($P=0.046$). In the BG group, the tissue integration score significantly increased from week 4 to week 16, and from week 8 to week 16 ($P=0.034$ and $P=0.041$, respectively).

Remaining membrane thickness

BG was thicker than CM at week 4 ($P=0.001$) (**Table 3**). The thickness of BG and CM significantly decreased between 4 and 8 weeks ($P=0.002$ and $P=0.001$, respectively); however, there was no significant difference between 8 and 16 weeks ($P>0.05$).

Remaining membrane area

The remaining membrane area was higher in the CM group than in the BG group at week 16 ($P=0.047$) (**Table 3**); however, there were no significant differences at weeks 4 and 8 ($P>0.05$). In both groups, the remaining membrane area significantly decreased between 4 and 8 weeks, and between 4 and 16 weeks (**Table 3**); however, there was no significant difference between 8 and 16 weeks ($P>0.05$).

Pseudoperiosteum

Pseudoperiosteum was present only in 5 samples of the 16-week BG group.

Table 3. Histomorphometric measurements at 4, 8, and 16 weeks after surgery

Variables	Time point (wk)	4 wk	8 wk	16 wk
Thickness (mm)	CM	0.53±0.09 ^{a,b)}	0.12±0.07	0.13±0.1
	BG	0.84±0.09 ^{a,b,c)}	0.3±0.19	0.14±0.05
Area (mm ²)	CM	2.16±0.48 ^{a,b)}	0.21±0.18	1.16±0.79 ^{c)}
	BG	3.41±1.11 ^{a,b)}	0.36±0.28	0.18±0.25

CM: crosslinked collagen membrane, BG: Bio-Gide.

Thickness: remaining absorbable membrane thickness, area: remaining absorbable membrane area.

^{a)}Significant intragroup difference between week 4 and week 8; ^{b)}Significant intragroup difference between week 4 and week 16; ^{c)}Significant intergroup difference at the same observation period.

DISCUSSION

Although collagen membranes are known to lose their barrier function following rapid degradation, some studies have indicated that the membrane becomes closely integrated with the surrounding tissues to provide a continuous bioactive role in bone regeneration [13,14]. Therefore, in this study, BG and CM were applied in a GBR model at 3 sequential time points up to 16 weeks to assess the progression of vascularization, tissue integration, tissue maturation and membrane degradation. The main findings were i) BG exhibited greater neovascularization, tissue integration, and tissue maturation than CM at 4, 8, and 16 weeks, ii) almost complete biodegradation of both membranes occurred between 4 to 8 weeks, and iii) at 16 weeks, a thickened band of mature fibrous tissues was formed in the space once occupied by BG, whereas the membrane remnants were still present in the CM group.

The importance of angiogenesis in GBR has been emphasized since the introduction of resorbable collagen membranes [15]. In the normal wound healing process, after the initial formation of a blood clot and granulation tissue in the defect space, the formation of a rich vascular supply has been shown to be crucial to osteoid formation and subsequent woven bone formation [16]. Although the vascular network is known to be mainly supplied by the alveolar bone at the defect site, an additional vascular supply from the overlying soft tissues may enhance healing and increase the rate of osteogenesis. Therefore, transmembraneous angiogenesis has been indicated to provide an additional healing source during the early formation of new bone by natural collagen membranes [12,17]. In this study, vascularization of BG increased significantly from week 4 to week 16. The CM group showed delayed vascularization in comparison to BG, resulting in a significant difference in the number of vessels after 16 weeks. It could be assumed that the lack of vascularization in the CM group might have been caused by the crosslinking of collagen. Related studies have also shown that neovascularization was negatively correlated with the extent of chemical cross-linking of the collagen matrix [12,18].

Tissue integration is an important criterion for absorbable barrier membranes to minimize immune responses and allow cellular proliferation around the membrane. Meanwhile, an integrated barrier membrane should ideally maintain the barrier function and cell occlusivity during the healing period. In this study, tissue integration was measured by the proximity between the barrier membrane and the surrounding tissues. BG was closely integrated with the surrounding tissues even at 4 weeks, whereas CM appeared to be separate from the adjacent tissues even at 16 weeks. These findings are similar to a previous study, in which increased levels of crosslinking were found to be negatively correlated with tissue integration [18]. Reduced tissue integration of crosslinked collagen membranes could be related to the release of toxic crosslinking agents from resorption of the membrane, which can alleviate negative tissue response. Compared with natural collagen membranes, crosslinked collagen membranes with an extended absorption time showed significantly more adverse events and less bone regeneration [19]. However, a preceding study using the current data showed that CM was superior to BG for new bone formation [20]. This may be due to the fact that CM still maintained a certain spatial shape at week 16, while BG began to degrade rapidly at week 4, resulting in the displacement or loss of bone graft materials, affecting bone regeneration. This also indicates that the membrane obtained by chemical crosslinking has a moderately long degradation time and appropriate biocompatibility, but is not conducive to tissue integration and angiogenesis [11].

The existence of a periosteum-like structure in the BG group at week 16 was a key finding of this study. A human autopsy study [21] also found periosteum-like structures at a site that had been grafted using BG, which seemed to last for more than 6 years after surgery. In this study, the tissue was found to contain small blood vessels, which could be assumed to supply blood to the defect site from the overlying tissues. In the BG group, the membrane appears to have been replaced by a highly vascular pseudoperiosteal tissue, which provided a biological barrier even after the collagen membrane was biodegraded. It may be speculated that this thickened layer of dense connective tissue might be the product of encapsulation and maturation of the tissues surrounding the integrated collagen membrane. This connective tissue structure should be studied further to reveal its biological activity in future studies.

This study had some limitations. Firstly, two commercially available barrier membranes with different collagen compositions and manufacturing techniques were used to represent crosslinked and non-crosslinked collagen membranes. Ideally, to properly assess the isolated effect of crosslinking, the same collagen membrane should be used with or without crosslinking. Secondly, the semi-quantitative and descriptive nature of the scoring system might have been subject to examiner bias. Measures were taken to prevent bias by blinding the examiners to the groups and involving multiple examiners to review the outcomes.

Although the BG membranes were rapidly biodegraded, they gradually became replaced by connective tissue with complete integration and maturation of the surrounding tissues to form dense periosteum-like connective tissue. However, the barrier function of BG membranes remains to be validated. In contrast, the CM membranes remained unresorbed longer and resulted in less vascularity and tissue integration than BG.

REFERENCES

1. Sanz-Sánchez I, Ortiz-Vigón A, Sanz-Martín I, Figuero E, Sanz M. Effectiveness of lateral bone augmentation on the alveolar crest dimension: a systematic review and meta-analysis. *J Dent Res* 2015;94 Suppl:128S-42S.
[PUBMED](#) | [CROSSREF](#)
2. Bunyaratavej P, Wang HL. Collagen membranes: a review. *J Periodontol* 2001;72:215-29.
[PUBMED](#) | [CROSSREF](#)
3. Gough JE, Scotchford CA, Downes S. Cytotoxicity of glutaraldehyde crosslinked collagen/poly(vinyl alcohol) films is by the mechanism of apoptosis. *J Biomed Mater Res* 2002;61:121-30.
[PUBMED](#) | [CROSSREF](#)
4. Ahn JJ, Kim HJ, Bae EB, Cho WT, Choi Y, Hwang SH, et al. Evaluation of 1-ethyl-3-(3-dimethylaminopropyl) carbodiimide cross-linked collagen membranes for guided bone regeneration in beagle dogs. *Materials (Basel)* 2020;13:E4599.
[PUBMED](#) | [CROSSREF](#)
5. Park JY, Jung IH, Kim YK, Lim HC, Lee JS, Jung UW, et al. Guided bone regeneration using 1-ethyl-3-(3-dimethylaminopropyl) carbodiimide (EDC)-cross-linked type-I collagen membrane with biphasic calcium phosphate at rabbit calvarial defects. *Biomater Res* 2015;19:15.
[PUBMED](#) | [CROSSREF](#)
6. Omar O, Elgali I, Dahlin C, Thomsen P. Barrier membranes: more than the barrier effect? *J Clin Periodontol* 2019;46 Suppl 21:103-23.
[PUBMED](#) | [CROSSREF](#)
7. Park JY, Song YW, Ko KA, Strauss FJ, Thoma DS, Lee JS. Effect of collagen membrane fixation on ridge volume stability and new bone formation following guided bone regeneration. *J Clin Periodontol* 2022;49:684-93.
[PUBMED](#) | [CROSSREF](#)

8. Urban IA, Montero E, Monje A, Sanz-Sánchez I. Effectiveness of vertical ridge augmentation interventions: a systematic review and meta-analysis. *J Clin Periodontol* 2019;46 Suppl 21:319-39.
[PUBMED](#) | [CROSSREF](#)
9. Jiménez García J, Berghezan S, Caramês JM, Dard MM, Marques DN. Effect of cross-linked vs non-cross-linked collagen membranes on bone: a systematic review. *J Periodontol Res* 2017;52:955-64.
[PUBMED](#) | [CROSSREF](#)
10. Naenni N, Lim HC, Strauss FJ, Jung RE, Hämmerle CH, Thoma DS. Local tissue effects of various barrier membranes in a rat subcutaneous model. *J Periodontal Implant Sci* 2020;50:327-39.
[PUBMED](#) | [CROSSREF](#)
11. Rothamel D, Schwarz F, Sager M, Herten M, Sculean A, Becker J. Biodegradation of differently cross-linked collagen membranes: an experimental study in the rat. *Clin Oral Implants Res* 2005;16:369-78.
[PUBMED](#) | [CROSSREF](#)
12. Schwarz F, Rothamel D, Herten M, Sager M, Becker J. Angiogenesis pattern of native and cross-linked collagen membranes: an immunohistochemical study in the rat. *Clin Oral Implants Res* 2006;17:403-9.
[PUBMED](#) | [CROSSREF](#)
13. Cha JK, Pla R, Vignoletti F, Jung UW, Sanz-Esporrin J, Sanz M. Immunohistochemical characteristics of lateral bone augmentation using different biomaterials around chronic peri-implant dehiscence defects: An experimental *in vivo* study. *Clin Oral Implants Res* 2021;32:569-80.
[PUBMED](#) | [CROSSREF](#)
14. Omar O, Dahlin A, Gasser A, Dahlin C. Tissue dynamics and regenerative outcome in two resorbable non-cross-linked collagen membranes for guided bone regeneration: a preclinical molecular and histological study *in vivo*. *Clin Oral Implants Res* 2018;29:7-19.
[PUBMED](#) | [CROSSREF](#)
15. Schmid J, Wallkamm B, Hämmerle CH, Gogolewski S, Lang NP. The significance of angiogenesis in guided bone regeneration. A case report of a rabbit experiment. *Clin Oral Implants Res* 1997;8:244-8.
[PUBMED](#) | [CROSSREF](#)
16. Cucchi A, Sartori M, Aldini NN, Vignudelli E, Corinaldesi G. A proposal of pseudo-periosteum classification after GBR by means of titanium-reinforced d-PTFE membranes or titanium meshes plus cross-linked collagen membranes. *Int J Periodont Restor Dent* 2019;39:e157-65.
[PUBMED](#) | [CROSSREF](#)
17. Schwarz F, Rothamel D, Herten M, Wüstefeld M, Sager M, Ferrari D, et al. Immunohistochemical characterization of guided bone regeneration at a dehiscence-type defect using different barrier membranes: an experimental study in dogs. *Clin Oral Implants Res* 2008;19:402-15.
[PUBMED](#) | [CROSSREF](#)
18. Thoma DS, Villar CC, Cochran DL, Hämmerle CH, Jung RE. Tissue integration of collagen-based matrices: an experimental study in mice. *Clin Oral Implants Res* 2012;23:1333-9.
[PUBMED](#) | [CROSSREF](#)
19. Tal H, Kozlovsky A, Artzi Z, Nemcovsky CE, Moses O. Long-term bio-degradation of cross-linked and non-cross-linked collagen barriers in human guided bone regeneration. *Clin Oral Implants Res* 2008;19:295-302.
[PUBMED](#) | [CROSSREF](#)
20. Lee JT, Cha JK, Kim S, Jung UW, Thoma DS, Jung RE. Lateral onlay grafting using different combinations of soft-type synthetic block grafts and resorbable collagen membranes: an experimental *in vivo* study. *Clin Oral Implants Res* 2020;31:303-14.
[PUBMED](#) | [CROSSREF](#)
21. Cha JK, Sanz M, Jung UW. Human autopsy study of peri-implant dehiscence defects with guided bone regeneration: a case report. *Int J Periodont Restor Dent* 2019;39:517-24.
[PUBMED](#) | [CROSSREF](#)